Corrosion of Mild Steel with Composite Alkyd Polyaniline-benzoate Coating

Ayad A. Salem, Branimir N. Grgur[*]

Faculty of Technology and Metallurgy, University of Belgrade, Karnegijeva 4, 11020 Belgrade, Serbia
[*]E-mail: BNGrgur@tmf.bg.ac.rs

The synthesis of the polyaniline in the emeraldine salt form by the procedure suggested by IUPAC is successful preformed. Emeraldine salt form is deprotonated with ammonium hydroxide and reprotonated with benzoic acid. Using the UV-visible spectroscopy the doping degree of 0.25 is estimated. The corrosion performances of the base coating and composite coating with 5 wt.% of polyaniline benzoate on mild steel are investigated by the means of linear polarization measurements and results are compared with *in site* determined iron concentrations in the corrosive media using ASTM 1,10-phenanthroline method and the corrosion current density is recalculated. Excellent agreement between these two methods is achieved. It is shown that composite containing polyaniline, offers an order of magnitude better corrosion protection than base coating, and more than three order of magnitude than pure mild steel.

1. INTRODUCTION

Conducting polymers or intrinsically conducting polymers (ICP's), are known as frontline area of investigations and potential materials for different technological applications including biosensors and gas-sensors [1,2], electrochromic devices [3], electromagnetic shielding [4], light emitting diodes and organic based electronics [5] photovoltaic applications [6], energy storage [7] *etc*. Among polypyrrole (PPy) [8], polythiophene (PT) [9], poly(p-phenylene) (PPP) [10,11], poly(3,4-ethylenedioxythiophene) (PEDOT), [12], the polyaniline (PANI) is one of the most extensively studied and applied conducting polymer because of its ease synthesis, low price of the monomer, relatively high electrical conductivity, oxidative properties, environmental stability *etc* [5,13]. Between above-mentioned applications, corrosion protection of different metals, and especially mild steel, is one of the well-studied field [14]. After pioneering work of DeBery [15], and Wessling [16], different researchers

groups [17-24] reported various views about the corrosion protection by thin film polyaniline coatings and the systems based on composite organic coating-polyaniline in powdered form as a filer. Huge dissipation of reported data could be connected with the applications of different synthesis routes used to prepare polyaniline powder. Hereafter, different role of the polyaniline in corrosion protection and various mechanisms are suggested to explain anticorrosion properties, like ennobling, barrier protection mechanisms or controlled inhibitor release [14]. A careful choice of the synthesis parameters could leads to an improvement in the anticorrosion properties of the coatings prepared using ICP's for metals and their alloys. Usually, chemical synthesis of the polyaniline in the emeraldine salt form using ammonium persulfate are conducted by adding different organic and inorganic acids in the reaction mixture, claiming that only used acid anion is doped in the polyaniline chain [25-28]. Nevertheless, in our point of view, under this synthetic condition, sulfate anions could be doped as well, for the reason that a significant amount of the sulfuric acid is released during synthesis. Consequently, to avoid this confusion, for the reproducibility, the well-established procedure of polyaniline synthesis as recommended by IUPAC [29] should be used, and the reprotonation of the polyaniline base route with corresponding acid will be the best method to obtain well defined polyaniline in the emeraldine salt form, as proposed by Stejskal et al. [30].

Hence, the aim of this work will be to use the procedure for synthesis of the polyaniline emeraldine salt according to recommended IUPAC procedure [29], deprotonate salt to form emeraldine base and to reprotonate base [30] to the well-defined salt with only one dopant. Such powder will be used to prepare composite coatings by simple procedure of mixing with commercial paint, and to investigate potential influence on the mild steel corrosion. In addition, the goal will be to eventually suggest the procedures to investigate corrosion protection of mild steel with composite base coating-polyaniline using different techniques and methods.

2. EXPERIMENTAL

The chemical synthesis of polyaniline is conducted according to the standard IUPAC procedures, recommended by Stejskal et al. [29]. To reduce the presence of residual aniline and to obtain the best yield of PANI, the ammonium persulfate-anilinium hydrochloride stoichiometric ratio of 1.25 is used as recommended. Anilinium hydrochloride is prepared by mixing 0.11 mol HCl (4 g or 13 cm^3 of 37 wt.% HCl, p.a. Merck) with 0.11 mol aniline monomer (10.23 g or 10.4 cm^3, p.a. Sigma Aldrich, previously distilled under reduced pressure), at room temperature in 250 cm^3 of distilled water. After stirring, 250 ml of 0.11 mol HCl contained 0.1375 mol (31.4 g) of ammonium persulfate is slowly added dropwise. After 24 h of stirring, the green powder is filtered, washed several times with 0.1 M HCl, distilled water and acetone, and dried overnight. The as synthesized polyaniline powder in the emeraldine salt form (ES-IUPAC) is treated with 1 M ammonium hydroxide for 24 hours to obtain the emeraldine base form (EB-IUPAC). After washing with distilled water and drying, the obtained emeraldine base powder (3 g) is treated with 150 cm^3 of 0.1 M benzoic acid (pK_a=4.202,

pH~2.6) for 24 hours at 70°C due to its low solubility at room temperature to produce the polyaniline-benzoate doped emeraldine salt [31].

The UV-vis spectra of the samples in powdered form dispersed in the water (~15 mg/20 cm^3) using ultrasound are recorded using a LLG uniSPEC 2 spectrophotometer.

As a base coating the commercial TESSAROL®-Helios, Slovenia, a primer paint for iron, based on an alkyd binder, with red pigments in the mixture of organic solvents (CAS No: 1174522-20-3, hydrocarbons, C9-C11, n-alkanes, isoalkanes, cyclics, < 2% aromatics, up to 30 wt.%), is used [32]. The composite coating is prepared by the mechanical mixing 10 g of base paint with 5 wt.% of well grinded polyaniline-benzoate powder, 0.335 g based on dry paint, with the particle size between 5 to 10 μm, determined by optical microscope. The base primer paint and composite coating are applied using a doctor-blade method on the properly cleaned mild steel (ANSI 1212) in the shape of cylinders inserted in plastic holder (to avoid edge effect) on the free circle side (2 cm^2) of the sample. The image of the sample holder, which is made to simultaneously measure two samples, is shown in Fig. 1. The corrosion of mild steel is investigated using the similar holder, but with one electrode.

Figure 1. Image of the samples holder used in the polarization investigations.

After drying in the air for 24 h, the coatings thickness are 60±5 μm, measured using Byko-test 4500 FE/NFe (Germany) coating thickness tester. The same procedure is applied on two 4 cm × 5 cm mild steel coupons, which back sides and the edges are protected with thick, ~200 μm, epoxy coating that are separately immersed in 200 cm^3 of 3% NaCl for 10 days.

The corrosion of the samples, using sample holder shown in Fig. 1, are investigated in 3% NaCl over time applying the ASTM International recommended linear polarization method for determination of the polarization resistance, R_p [33] from the polarization measurements, using Gamry PC3 potentiostat controlled by a computer. The platinum counter electrode and saturated calomel as a reference electrode are used. The rate of the corrosion of two 4 cm × 5 cm mild steel samples with base and composite coating, as a concentration of iron in 200 cm^3 of 3% NaCl solution, are determined after 10 days of corrosion using the slightly modified ASTM International 1,10-phenanthroline standard method [34]. In a typical procedure, after 10 days of corrosion, samples are taken from corrosion

media, and 10 cm^3 concentrated HCl acid is added to dissolve eventually present insoluble corrosion products. The 10 cm^3 of stack solutions is transferred to 100 cm^3 volumetric flask, then 1 cm^3 of the hydroxylamine solution (100 g dm^3), 10 cm^3 of the 1,10-phenanthroline solution (1 g dm^3) and 8 cm^3 of the sodium acetate solution (1.2 M) is added, respectively. For the preparation of the iron standard solutions, the ferrous ammonium sulfate hexahydrate, $(NH_4)_2(SO_4)_2 \times 6H_2O$ (Aldrich, p.a.) is used. The concentrations are determined measuring the UV-visible absorbance at 508 nm of standard and investigated solutions, using a LLG uniSPEC 2 spectrophotometer. The quality of the coatings after corrosion are investigated using optical microscopy, and optical micrographs are obtained with an optical microscope Olympus CX41 connected to a personal computer.

3. RESULTS AND DISCUSSION

3.1. Characterization of the polyaniline

The UV-visible spectra of different PANI samples dispersed in water from 190 to 1100 nm are shown in Fig. 2. For as synthetized polyaniline in the emeraldine salt form (ES-IUPAC; doping degree: $y = 0.5$) the absorption peak at ~350 nm is assigned to the π–π^* transition within the benzenoid ring (B), peak at ~462 nm could be assigned to polaron - π^* transition within doped quinoid (Q) structure [35], followed by broad tail associated with polaronic structures. The spectra of the polyaniline in emeraldine base form (EB-IUPAC) among peak at 350 nm, has a strong peak at ~700 nm, which is attributed to the molecular excitation associated with the quinoid-imine structure [36]. The ratio of the absorption at 350 nm and at 700 nm, is equal to one, suggesting the same numbers of Q and B repeated units in the polymer chain, or pure half oxidized emeraldin structure.
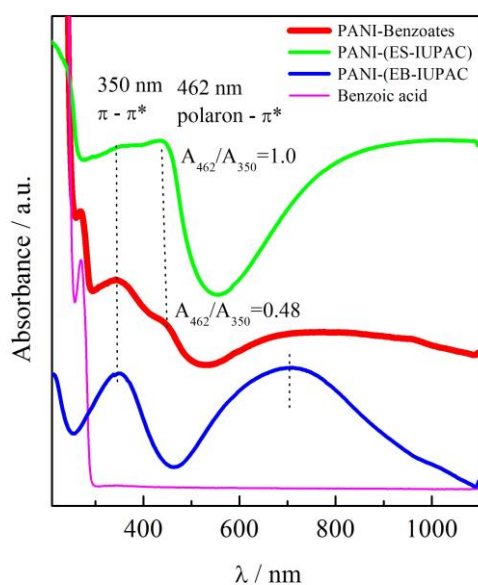

Figure 2. The UV-vis spectra of the PANI samples ultrasonically dispersed in distilled water (15 mg/20 cm^3).

The strong sharp peak at 273 nm of the chemically doped (reprotonated) sample correspond to the absorption of benzoic acid, which absorption spectra is also shown in Fig. 1, and is ascribed to the π–π* transition in the benzoates, suggesting successful doping of emeraldine base. The strong peak at 350 nm is generated by the π–π* transition in the PANI chains. Broad tail above ~500 nm is associated with polaronic structures in the polyaniline [35,36]. The appearance of the absorption at 462 nm, is associated with the doping of the quinoid (Q) structures with benzoate anions.

According to the UV-visible spectra, shown in Fig. 2, it can be concluded that interconversion of polyaniline emeraldine base to emeraldine salt according to the scheme shown in Fig. 3 is successful. However, from the ratio of A_{462}/A_{350} peaks, marked in Fig. 2, which for the as synthetized sample is equal to one, it could be also concluded that benzoate doped polymer has a lower oxidation state than as synthesized polyaniline. Assuming that doping degree (number of anions per polymer units) of as synthetized sample is $y = 0.5$, two anions per four monomer units, the doping degree of benzoate doped polyaniline is estimated to ~0.24 or only one anions per four monomer units.
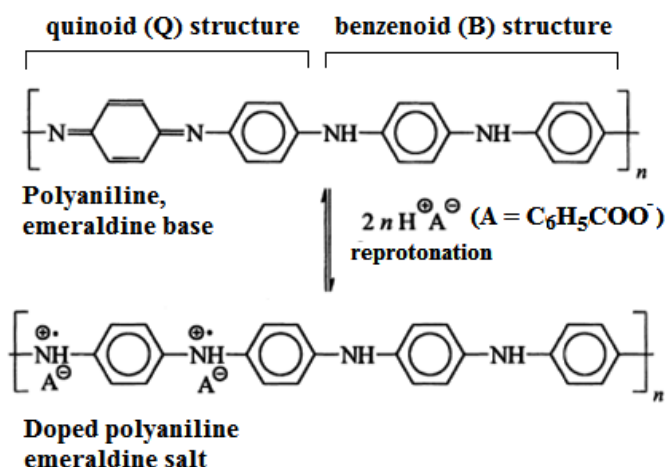

Figure 3. Schematic presentation of the reprotonation of the polyaniline emeraldine base to emeraldine salt with benzoic acid.

3.2. Corrosion investigations

Mild steel corrode in the saline solutions under the diffusion controlled oxygen reduction reaction, as can be seen in Fig. 4, according to the equation:

$$O_2 + OH^- + 4e = H_2O \qquad (1)$$

as the cathodic reaction, while the anodic reaction is dissolution of the iron:

$$Fe = Fe^{2+} + 2e \qquad (2)$$

From Fig. 4, can be also seen that anodic part of the polarization curve is characterized with two Tafel slopes, *b*, of 78 mV dec[-1] at low current density region, and 135 mV dec[-1] at high current density region. From intercept of Tafel slope from low current density region on the corrosion potential of –0.642 V, the corrosion current density of 12 µA cm^{-2} is obtained. Inset of Fig. 4 shows the polarization in the linear region, where slopes of $E = f(j)$ represents polarization resistance:

$$R_p = \left(\frac{\partial E}{\partial j} \right)_{\eta < \pm 20\,\mathrm{mV}} \tag{3}$$
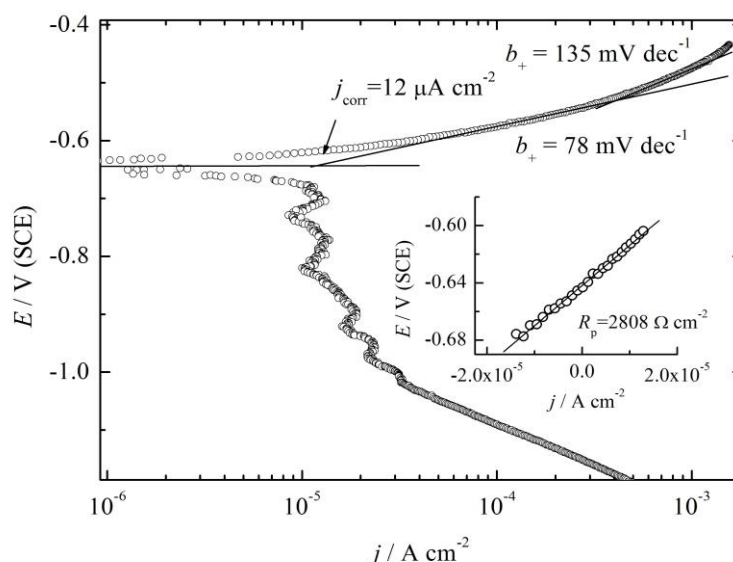

Figure 4. Polarization curve ($v = 1$ mV s^{-1}) of mild steel in the aerated 3% NaCl. Inset: the linear polarization region and determination of the polarization resistance R_p.

The corrosion current density can be obtained from determined R_p using the Stern-Geary equation [37,38]:

$$j_{corr} = \frac{b_+ b_-}{2.3(b_+ + b_-)R_p} \tag{4}$$

or in the case of diffusion limitations when $b_- \rightarrow \infty$, of the cathodic reaction:

$$j_{corr} = \frac{b_+}{2.3R_p} \tag{5}$$

For the determined R_p of 2808 Ω cm[2], inset in Fig. 4, corresponding calculated current density, Eq. 5, is 12.1 µA cm^{-2}, which is an identical value as obtained from the Tafel extrapolation.

Using the same approach, the polarization measurements over the immersion times in 3% NaCl are performed on the samples covered with base and composite coating. In Fig. 5a some of the measured polarization curves of the investigated samples in the form of Tafel plots for better visibility, ~±50 mV around the corrosion potential during few characteristics times are shown. Fig. 5b shows as an example, a linear polarization lines from which the polarization resistance is determined after 1 day of immersion in 3% NaCl. The same analysis is applied for all measured polarization curves over the times. From Fig. 5a, can be seen that composite coating possess more positive corrosion potential and lower ranges of corrosion current densities than base coating. The deterioration of the base coating characteristic is observed after ten days, while the composite coating last for twenty-five days.
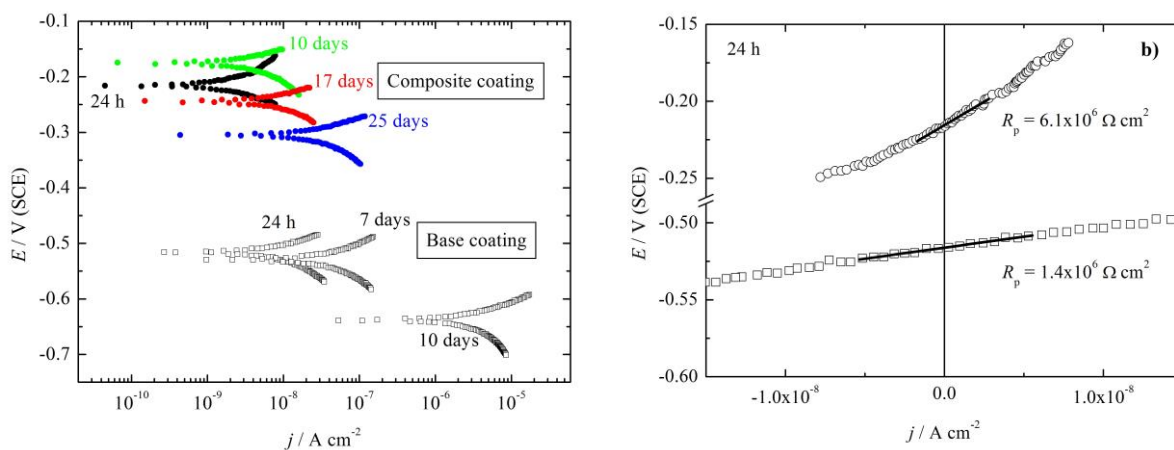

Figure 5. a) Representative polarization curves ($v = 1$ mV s^{-1}) of investigated samples over time in 3% NaCl. b) Examples of the polarization resistance, R_p, determination from the linear polarization lines after 24 h of immersion in 3% NaCl; (□) base coating, and (○) composite coating with 5 wt.% of polyanilin-benzoate powder.

In Fig. 6 the dependence of the determined polarization resistance for all measured times of the investigated samples are shown. For the comparison the determined polarization resistance (~3×10^3 Ω cm^2) of mild steel during five days are also shown. During firs two days of immersion base coatings shows decrease of the polarization resistance from 3×10^6 Ω cm^2 to ~3×10^5 Ω cm^2 as a consequence of the electrolyte uptake, followed by a plateau over next eight days. This period can be assigned to the macro-pores development and penetration of the electrolyte in the coating connected with good protection performances [39]. After ten days, the electrolyte is in contact with the metal surface in the pores that leads to the loss of adhesion and to delamination of the coating. This is caused by the accumulations of the hydroxyl ions in to pores, increases of the pH to the very high values and degradations of the polymer to metal bonds and loss of the adhesion [40]. The composite coatings shows much better polarization characteristics. Initially a small increase of the polarization resistance is observed, followed by a plateau with an order of magnitude higher value than base coating, and retain the value over 4×10^5 Ω cm^2 even after 25 days of immersion. In comparison with mild steel, it can be seen that the polarization resistance is more than three order of magnitude higher.
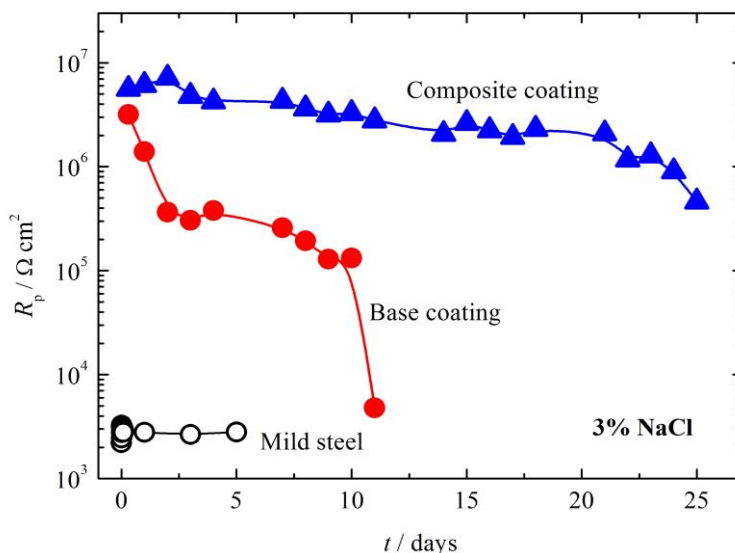
Figure 6. The dependence of the determined polarization resistance, R_p, from the polarization measurements over time of the investigated samples.

From the determined values of the polarization resistances, presented in Fig. 6, assuming that anodic and cathodic reaction through pores of the coated mild steel are the same as for the uncoated mild steel sample, the corrosion current density can be estimated using the Eq. 5 and the value of the anodic Tafel slope of 78 mV dec^{-1}. The calculated values of the corrosion current densities are shown in Fig. 7. It is obvious that composite coating has superior characteristics than base coating, and a three order of magnitude lower corrosion current densities than pure mild steel, which is shown for comparisons.
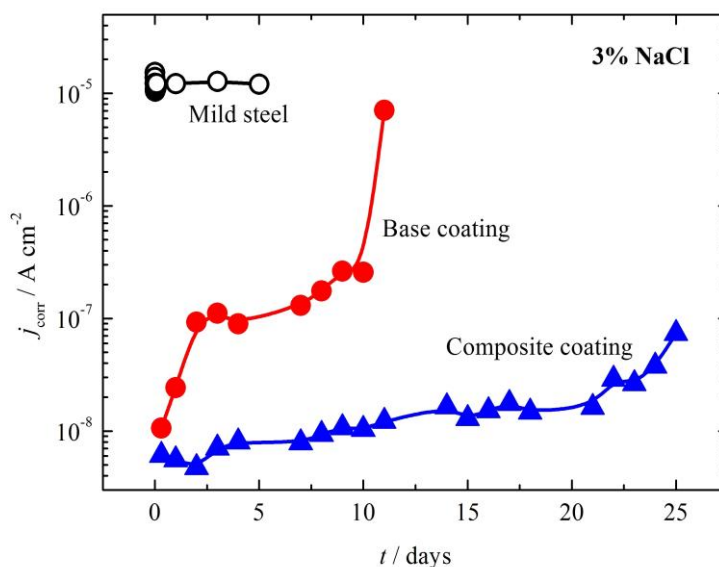
Figure 7. Estimated corrosion current densities using data from Fig. 6 and Eq. 5 in 3% NaCl for the investigated samples over time.

The corrosion rate of the higher area samples after ten days of immersion in 3% NaCl is determined using the 1,10-phenanthroline method. In the inset of Fig. 8, the dependence of the absorption on standard iron solutions with different concentrations is shown. The linear dependence of the absorption of standard solutions at 508 nm is in accordance with Lambert–Beer law. The absorption can be given as $A = 1.68\ c(Fe^{2+})$, so the iron concentration is $c(Fe^{2+}) = A/1.68$. The absorption maximum for the solution in which base coating corroded is 0.0855, which correspond to 0.051 mg per 10 cm^3 of the investigated samples or 1.02 mg of iron in 200 cm^3. For the solution in which composite coating corroded the absorption maximum is 0.014, corresponding to 0.167 mg per 200 cm^3 of solution. Using the Faraday law in the form:

$$j_{corr} = \frac{I_{corr}}{A} = \frac{c(Fe^{2+}) \times n \times F}{t \times M(Fe)} \qquad (6)$$

where, A is the surface area of the samples, 20 cm^2, $c(Fe^{2+})$ is mass of iron in grams (per 200 cm^3), F is Faraday constant (26.8 Ah mol^{-1}) and t immersion time in hours, the corrosion current density of 2×10^{-7} A cm^{-2} for the base coating, and 3.3×10^{-8} A cm^{-2} for the composite coating are determined. Very similar value of 2.7×10^{-7} A cm^{-2} for the base coating, and 1.1×10^{-8} A cm^{-2} for the composite coating are obtained using the linear polarization method (compare the data in Fig. 7, after ten days).
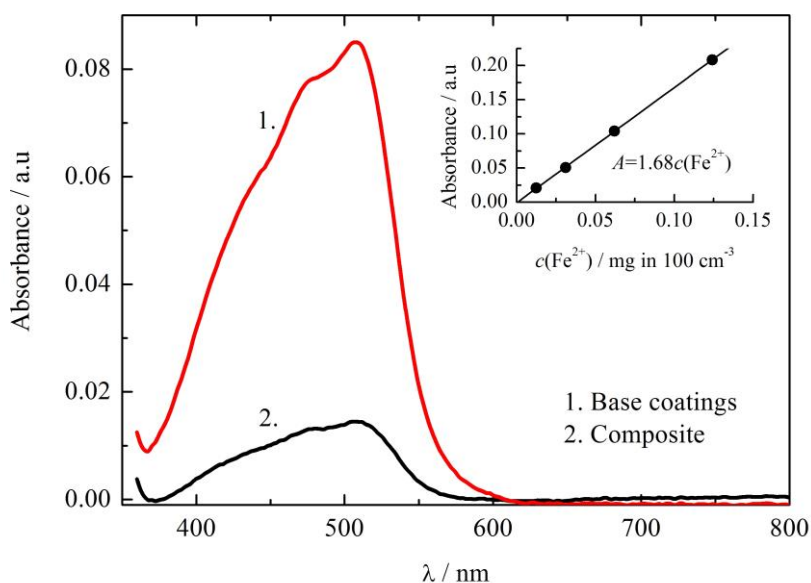

Figure 8. UV-visible spectra of the corrosion media samples after ten days of corrosion. Inset: Absorption at 508 nm of standard iron solutions.

The base and composite coating containing 5 wt.% of polyaniline benzoate are also investigated with optical microscope after ten days of immersion in a 3% NaCl solution. A micrograph image of the samples after the corrosion test is shown in Fig. 9. The base coating corroded and forms blisters and large delamination areas. However, the base coating with 5 wt.% of polyaniline remained practically unchanged, showing the superior anticorrosion characteristics.
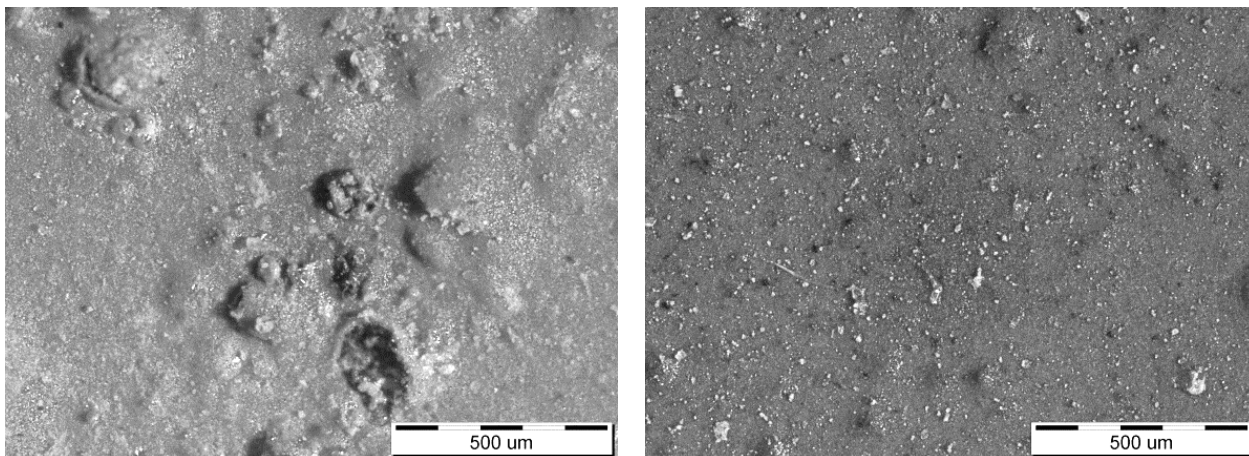
Figure 9. The micrographs of the samples after ten days of immersion in 3% NaCl. Left: base coating; right: base coating with + 5 wt% PANI-benzoate.

Similar results of the base coatings corrosion stability improvement are obtained by different authors [14, 17-25], and explained mainly by the ennobling of the mild steel in contacts and interactions with polyaniline [41]. However, as previously explained, delamination of the base coating is initiated by the accumulations of the hydroxyl ions in to pores *via* reaction given by Eq. 1, and increases of the pH to the very high values. Therefore, we would like to propose an alternative view that the main differences in the improved corrosion performance of the composite coating is in the oxygen reduction reaction mechanism. In comparisons with base coating, it is possible that in the pores of composite coating oxygen reduction could be mainly via hydrogen peroxide path (two-electron path), on the exposed polyaniline particles, as shown by few authors for some conducting polymers [42-45]:

$$(PANI): O_2 + H_2O + 2e \rightarrow HO_2^- + OH^- \tag{4}$$

Therefore, during this reaction only one hydroxyl ions is released, instead of four, that suppress a high increase in pH in to the pores, and prolong delamination effect. This could be an additional effect among well-elaborated ennobling effect [41] in the role of the polyaniline.

4. CONCLUSION

The reprotonation of the polyaniline base obtained following the standard IUPAC procedure is successful demonstrated. UV-visible techniques can be applied to determine the oxidation states of the reprotonated samples. Commercial paint is modified as a composite paint by addition of 5 wt.% benzoic acid reprotonated polyaniline powder. The linear polarization measurements are effectively performed in the polarization resistance and corrosion current density determination over time, suggesting that such investigations will be good indication of corrosion behavior of the systems, and

can be used in the further study. Using the UV-visible studies of the corrosion products, based on ASTM 1,10-phenanthroline method, the corrosion current density practically identical to obtained ones by linear polarization method are determined. Based on the performed corrosion experiments and microscopic observations, it is concluded that composite coatings based on commercial paint with addition of the polyaniline-doped with benzoate anions shows much better protection of the mild steel than base commercial coating, preventing the blister formation and coating delamination after prolonged periods. Among other mechanisms in the improvement of base coatings corrosion characteristics, it is suggested that oxygen reduction reaction could proceed via two-electron hydrogen peroxide path on polyaniline particles, releasing only one hydroxil ions instead of four, prolonging time before coating delamination.

References

1. I. Fratoddi, I. Venditti, C. Cametti and M.V. Russo, *Sens. Actuators B*, 220 (2015) 534.
2. H. Yoon, Nanomaterials, 3 (2013) 524.
3. A. Medrano-Solís, M. E. Nicho and F. Hernández-Guzmán, *J. Mater. Sci. Mater. Electron.*, 28 (3) (2017) 2471.
4. A. Pande, P. Gairola, P. Sambyal, S.P. Gairola, V. Kumar, K. Singh and S.K. Dhawan, *Mater. Chem. Phys.*, 189 (2017) 22.
5. K.M. Molapo, P.M. Ndangili, R.F. Ajayi, G. Mbambisa, S.M. Mailu, N. Njomo, M. Masikini, P. Baker and E.I. Iwuoha, *Int. J. Electrochem. Sci.*, 7 (2012) 11859.
6. H. S. Nalwa, Handbook of Organic Conductive Materials and Polymers, Wiley (1997) New York.
7. R. Holze and Y.P. Wu, *Electrochim. Acta*, 122 (2014) 93.
8. N. Su, H.B. Li, S.J. Yuan, S.P. Yi and E.Q. Yin, *eXPRESS Poly. Lett.*, 6 (9) (2012) 697.
9. S. Das, D.P. Chatterjee, R. Ghosh and Arun K. Nandi, *RSC Adv.*, 5 (2015) 20160.
10. A.J. Blayney, I.F. Perepichka, F. Wuld, and D.F Perepichka, *Isr. J. Chem.*, 54 (5-6) (2014). 674.
11. B. Guler, H. Akbulut, F.B. Barlas, C. Geyik, D.O. Demirkol, A.M. Senisik, H.A. Arican, H. Coskunol, S. Timur and Y. Yagci, *Macromol Biosci.*, 16 (5) (2016) 730.
12. K. Sun, S. Zhang, P. Li, Y. Xia, X. Zhang, D. Du, F.H. Isikgor and J. Ouyang, *J. Mater. Sci. Mater. Electron.*, 26 (7) (2015) 4438.
13. G. Ćirić-Marjanović, *Synth. Met.,* 177 (2013) 1.
14. P.P. Deshpande, N.G. Jadhav, V.J. Gelling and D. Sazou, *J. Coat. Technol. Res.*, 11 (4) (2014) 473.
15. D.W. DeBerry, *J. Electrochem. Soc.,* 132 (5) (1985) 1022.
16. B. Wessling, *Adv. Mater.*, 6 (3) (1994) 226.
17. B.A. Abd-El-Nabey, O.A. Abdullatef, G.A. El-Naggar, E.A. Matter and R. M. Salman, *Int. J. Electrochem. Sci.*, 11 (2016) 2721.
18. O. Kazum and M.B Kannan, *Surf. Eng.*, 32 (2016) 607.
19. S. Qiu, C. Chen, M. Cui, W Li, H. Zhao and L. Wang, *App. Surf. Sci.*, 407 (2017) 213.

20. U.A. Samad, M.A. Alam, El-S.M. Sherif, O. Alothman, A.H. Seikh and S. Al-Zahrani, *Int. J. Electrochem. Sci.*, 10 (2015) 5599.
21. M. Rohwerder, *Int. J. Mater. Res.*, 100 (10) (2009) 1331.
22. M. Khan, A.U. Chaudhry, S. Hashim, M.K. Zahoor and M.Z. Iqbal, *J. Coat. Technol. Res.*, 11 (4) (2014) 473.
23. T. Ohtsuka, *Int. J. Corr.*, 2012 (2012) 7.
24. R.M. Bandeira, J. van Drunen, G. Tremiliosi-Filho, J.R. dos Santos, and J.M.E. de Matos, *Prog. Org. Coat.*, 106 (2017) 50.
25. M. Kohl and A. Kalendová, *Prog. Org. Coat.*, 86 (2015) 96.
26. T. Li, Z. Qin, B. Liang, F. Tian, J. Zhao, N. Liu and M. Zhu, *Electrochim. Acta*, 177 (2015) 343.
27. S. Pour-Ali, C. Dehghanian and A. Kosari, *Corr. Sci.*, 85 (2014) 204.
28. M.V. Kulkarni, A.K. Viswanath, R. Marimuthu and T. Seth, *J. Polym. Sci. A Polym. Chem.*, 42 (8) (2004) 2043.
29. J. Stejskal and R. G. Gilbert, *Pure Appl. Chem.,* 74 (5) (2002) 857.
30. J. Stejskal, J. Prokeš and M. Trchová, *React. Funct. Polym,*. 68 (2008) 1355.
31. B.N. Grgur, A.R. Elkais, M.M. Gvozdenović, S.Z. Drmanić, T.Lj. Trišović and B.Z. Jugović, *Prog. Org. Coat.*, 79 (2015) 17.
32. https://www.helios-deco.com/en/products/metal-coatings/?use=&surface=0
33. ASTM Designation: G 59 – 97, Standard test method for conducting potentiodynamic polarization resistance measurements, 2014.
34. ASTM, Designation: E 394 – 00, Standard test method for iron in trace quantities using the 1,10-phenanthroline method, 2000.
35. E. Jin, N. Liu, X. Lu and W. Zhang*, Chem. Lett.* 36 (2007) 1288.
36. J.E. de Albuquerque L.H.C. Mattoso, R.M. Faria, J.G. Masters and A.G. MacDiarmid, *Synth. Met.* 146 (2004) 1.
37. M. Stern and A. L. Geary, *J. Electrochem. Soc.*, 104(1) (1957) 56.
38. M. Stern, Corrosion, 14, (9) (1958) 440t.
39. J.B. Bajat, V.B. Mišković-Stanković, M.D. Maksimović, D.M. Dražić and S. Zec, *Electrochim. Acta,* 47 (2002) 4101.
40. S.B. Lyon, R. Bingham and D.J. Mills, *Prog. Org. Coat.,* 102 (2017) 2.
41. M.P. Sokolova, M.A. Smirnov, I.A. Kasatkin, I.Yu. Dmitriev, N.N. Saprykina, A.M. Toikka, E. Lahderanta and G.K. Elyashevich, *Int. J. Poly. Sci.*, 2017 (2017), Article ID 6904862.
42. V.G. Khomenko, V.Z. Barsukov, A.S. Katashinskii, *Electrochim. Acta,* 50 (2005) 1675.
43. V.G. Khomenko, K.V. Lykhnytskyi, V.Z. Barsukov, *Electrochim. Acta*, 104 (2013) 391.
44. B.N. Grgur, *Synth. Met*., 187 (1) (2014) 57.
45. B.N. Grgur, *J. Power Sources*, 272 (2014) 1053.